Genetics: Early Online, published on May 11, 2017 as 10.1534/genetics.116.196881

# An evolutionarily conserved role of Presenilin in neuronal protection in the aging *Drosophila* brain

Jongkyun Kang[*], Sarah Shin[*], Norbert Perrimon[†,‡,1], and Jie Shen[*,§,1]

[*]Department of Neurology, Brigham and Women's Hospital, Harvard Medical School, Boston, MA, USA

[†]Department of Genetics, Harvard Medical School, Boston, MA, USA

[‡]Howard Hughes Medical Institute, Harvard Medical School, Boston, USA

[§]Program in Neuroscience, Harvard Medical School, Boston, USA

# Presenilin in *Drosophila* adult brains

**Keywords**: γ-secretase, Alzheimer's disease, conditional knockdown, shRNA, brain

[1]Corresponding authors:

Norbert Perrimon, Department of Genetics, Harvard Medical School, New Research Building, Room 336G, 77 Avenue Louis Pasteur, Boston, MA 02115. Email: perrimon@receptor.med.harvard.edu

Jie Shen, Department of Neurology, Brigham and Women's Hospital, Harvard Medical School, New Research Building 636E, 77 Avenue Louis Pasteur, Boston, MA 02115. Email: jshen@bwh.harvard.edu

## Abstract

Mutations in the *Presenilin* genes are the major genetic cause of Alzheimer's disease. Presenilin and Nicastrin are essential components of γ-secretase, a multi-subunit protease that cleaves Type I transmembrane proteins. Genetic studies in mice previously demonstrated that conditional inactivation of Presenilin or Nicastrin in excitatory neurons of the postnatal forebrain results in memory deficits, synaptic impairment and age-dependent neurodegeneration. The roles of *Drosophila Presenilin* (*Psn*) and *Nicastrin* (*Nct*) in the adult fly brain, however, are unknown. To knockdown (KD) *Psn* or *Nct* selectively in neurons of the adult brain, we generated multiple shRNA lines. Using a ubiquitous driver, these shRNA lines resulted in 80-90% reduction of mRNA and pupal lethality, a phenotype that is shared with *Psn* and *Nct* mutants carrying nonsense mutations. Furthermore, expression of these shRNAs in the wing disc caused notching wing phenotypes, which are also shared with *Psn* and *Nct* mutants. Similar to *Nct*, neuron-specific *Psn* KD using two independent shRNA lines led to early mortality and rough eye phenotypes, which were rescued by a fly *Psn* transgene. Interestingly, conditional KD (cKD) of *Psn* or *Nct* in adult neurons using the *elav-Gal4* and *tubulin-Gal80$^{ts}$* system caused shortened lifespan, climbing defects, increases in apoptosis and age-dependent neurodegeneration. Together, these findings demonstrate that similar to their mammalian counterparts, *Drosophila* Psn and Nct are required for neuronal survival during aging and normal lifespan, highlighting an evolutionarily conserved role of Presenilin in neuronal protection in the aging brain.

## Introduction

Presenilin (PS) is the catalytic subunit of the γ-secretase complex, which also contains Nicastrin (Nct) and cleaves type I transmembrane proteins, such as the Notch receptors (DE STROOPER *et al.* 1999; SONG *et al.* 1999; STRUHL and GREENWALD 1999; LI *et al.* 2000; YU *et al.* 2000; BAI *et al.* 2015). The *Presenilin-1* (*PSEN1*) and *Presenilin-2* genes were identified as the major genes linked to familial Alzheimer's disease (FAD) (LEVY-LAHAD *et al.* 1995; ROGAEV *et al.* 1995; SCHELLENBERG 1995). Genetic studies in mice have demonstrated that in the developing brain, PS regulates neurogenesis and cell-fate decisions through the Notch signaling pathway (SHEN *et al.* 1997; HANDLER *et al.* 2000; KIM and SHEN 2008), and that deficiency of *PS* or *Nct* results in early embryonic lethality (DONOVIEL *et al.* 1999; NGUYEN *et al.* 2006). Conditional gene targeting further demonstrated that PS and Nct are required for normal learning and memory, synaptic plasticity and neuronal survival in the mouse cerebral cortex (YU *et al.* 2001; BEGLOPOULOS *et al.* 2004; FENG *et al.* 2004; SAURA *et al.* 2004; TABUCHI *et al.* 2009; ZHANG *et al.* 2009; WINES-SAMUELSON *et al.* 2010; LEE *et al.* 2014; WATANABE *et al.* 2014).

*Drosophila Presenilin* (*Psn*) and *Nicastrin* (*Nct*) share high sequence homology with their human and mouse counterparts (HONG and KOO 1997; YU *et al.* 2000). Loss-of-function mutations in *Drosophila Psn* cause pupal lethality and Notch-like phenotypes, such as maternal neurogenic effects, loss of lateral inhibition within proneural cell clusters, and absence of wing margin formation (STRUHL and GREENWALD 1999; YE *et al.* 1999). Loss-of-function mutations in *Nct* also cause pupal lethality, and abolish Psn accumulation and Psn-dependent intramembrane cleavage of Notch (CHUNG and STRUHL 2001; HU *et al.* 2002). Genetic modifier screens of Notch-like phenotypes in *Psn* loss-of-function mutants also confirmed the genetic interaction between *Psn* and *Nct* in the *Drosophila* eye and wing (MAHONEY *et al.* 2006).

However, the pupal lethality of *Psn* and *Nct* mutants precluded studies of their functions in mature neurons of the adult brain. As a result, the consequences of Psn or Nct inactivation in adult neurons of the fly remain unknown.

In this study, we developed multiple shRNA lines targeting *Psn* or *Nct*. Using the *Act5c-Gal4* driver, we found that ubiquitous *Psn* or *Nct* knockdown (KD) in all cells leads to an ~80-90% reduction of *Psn* or *Nct* mRNA and pupal lethality, similar to homozygous null mutant flies (LUKINOVA *et al.* 1999; STRUHL and GREENWALD 1999; HU *et al.* 2002). Selective *Psn* or *Nct* KD in wing marginal discs caused notching phenotypes in the adult wing, further confirming that these *Psn* and *Nct* shRNA lines effectively suppress *Psn* and *Nct* function, respectively. Similar to *Nct*, neuron-specific *Psn* KD under the control of the *elav-Gal4* driver led to developmental defects with dramatic early mortality, severe climbing defects, and rough eye phenotypes. Expression of a fly *Psn* transgene rescued the early mortality and rough eye phenotypes of neuron-specific *Psn* KD. Strikingly, adult neuron-specific *Psn* or *Nct* conditional KD (cKD) flies using the *elav-Gal4/tub-Gal80$^{ts}$* system, which permits inducible expression of shRNAs in adult neurons, displayed shortened lifespan, climbing defects, increases in apoptosis, and age-dependent neurodegeneration. Together, these findings demonstrate that similar to their mammalian orthologs, *Drosophila Psn* and *Nct* are required for adult neuronal survival during aging and normal lifespan, highlighting an evolutionally conserved role of Presenilin in neuronal protection in the aging brain.

## Materials and Methods

### Generation of *Psn* and *Nct* shRNA transgenic flies

We newly generated *UAS-shRNA* lines against *Psn* (*shPsn1, 2, 3, 4*) and *Nct* (*shNct1, 2, 3*) as described (NI *et al.* 2011), which are different from those available at TRiP. Briefly, shRNA target regions were selected using a Perl program as described previously (VERT *et al.* 2006), and we avoided the 5' and 3' UTRs and the regions that have more than 15 bp match to other *Drosophila* transcripts to reduce the risk of off-target effects. The annealed top and bottom oligos containing the 21 bp shRNA target sequences against *Psn* and *Nct* were subcloned into pWALIUM20 (TRiP) vector following the UAS sequence. The sequences of the oligos used to generate *UAS-shPsn* and *UAS-shNct* transgenic flies are included in Table S1. As described previously (GROTH *et al.* 2004; VENKEN *et al.* 2006; MARKSTEIN *et al.* 2008), each transgene was injected into embryos for targeted phiC31-mediated integration at genomic attP landing sites on the second (attP16 or attP40) or third (attP2 or VK0027) chromosomes.

### Crosses and culture conditions

Flies were raised on standard cornmeal media, and maintained at either 22 or 25ºC and 40-60% relative humidity. Control flies in all experiments were as closely related to the experimental transgenic flies as possible. Typically, *UAS-shPsn* or *UAS-shNct* and Gal4 transgenic flies were crossed with $w^{1118}$ (Bloomington *Drosophila* Stock Center: BL5905) or *P(CarryP)attP2* (BL36303) to generate the heterozygous alleles of the *UAS-shRNA* or Gal4 transgene. We used ubiquitous (*Act5C-Gal4*), wing-specific (*c96-Gal4*) or neuron-specific (*elav-Gal4*$^{c155}$) drivers to generate *Psn* or *Nct* KD; female Gal4 transgenic flies were crossed with male *UAS-shRNA* flies. For the rescue experiments, *elav-Gal4/FM6;; UAS-shPsn2/TM6B* female flies

were crossed with male flies of human *UAS-hPSEN1* or *Drosophila UAS-Psn+14*. The progeny with the desired genotype (*elav-Gal4/+ (or y);; UAS-shPsn2/UAS-hPSEN1 or UAS-Psn+14*) was collected based on the absence of genetic markers in the FM6 and TM6B balancers.

To generate adult neuron-specific *Psn* or *Nct* cKD flies, *elav-Gal4;; tub-Gal80$^{ts}$* females were crossed with *UAS-shPsn2* or *UAS-shNct2* male flies at a permissive temperature of 22ºC and maintained at 22ºC until adulthood, then male offspring (*elav-Gal4/y;; tub-Gal80$^{ts}$/UAS-shPsn2* or *UAS-shNct2*) were collected and shifted to a restrictive temperature of 27ºC until the end of each experiment. To generate adult neuron-specific *Psn/Nct* cKD flies, *elav-Gal4;; tub-Gal80$^{ts}$, UAS-shPsn2/TM6B* females were crossed with *UAS-shNct2* male flies at 22ºC and maintained at 22ºC until adulthood, then male offspring (*elav-Gal4/y;; tub-Gal80$^{ts}$, UAS-shPsn2/UAS-shNct2*) were collected and shifted to 27ºC until the end of each experiment. All stocks were obtained from the Bloomington *Drosophila* Stock Center unless otherwise indicated.

**Quantitative RT-PCR (qRT-PCR)**

Five 3$^{rd}$ instar larvae were washed twice in RNase free PBS and collected in lysis buffer. Fifteen 3$^{rd}$ instar larval brains were dissected in RNase free PBS and homogenized in lysis buffer using a homogenizing blender (Next Advance). For adult fly RNA extraction, adult flies were collected and frozen immediately in liquid nitrogen. Five whole adult bodies were used for total RNA extraction. Twenty adult heads were removed from bodies by vortexing and then collected. Total RNA was extracted according to the manufacturer's instructions (Quick-RNA$^{TM}$ MicroPrep; Zymo Research). The eluted total RNA was reverse transcribed using iScript$^{TM}$ Select cDNA Synthesis Kit (Bio-Rad) with gene specific primers: 5'-TATAAACACCTGCTTGGCCG-3' for *Psn*, 5'-CGTGCACTGAACTGTGACCA-3' for *Nct* and 5'-GACAATCTCCTTGCGCTTCT-3' for *rp49*. Real-time qPCR was performed with

ViiA™ 7 Real-Time PCR System (ThermoFisher Scientific) using PowerUP SYBR Green Master Mix (ThermoFisher Scientific) with the following primers: for *Psn*, 5'-TCCCATCCTCGACAGAATCA-3' and 5'-TATGCCACGTTCTTCTTGCC-3'; for *Nct*, 5'-GACTTCATGCTGGACATCGG-3' and 5'-TTGCTGAGCCAAAGTCGTTC-3'; for *rp49*, 5'-AAGCGGCGACGCACTCTGTT-3' and 5'-GCCCAGCATACAGGCCCAAG-3'. The level of *rp49* mRNA was evaluated as an internal control for the total mRNA quantity in each sample. Data were analyzed with Microsoft Excel and Prism. More than four independent experiments were done for each analysis.

**Adult viability and lifespan analysis**

Fly viability was assessed by collecting and gently transferring twenty 3rd instar larvae to fresh vials at 25 °C. The total number of eclosed adult flies from the pupal cases was scored. Viability was calculated by dividing the total number of flies by the total number of pupae, and shown as the percentage of pupae surviving to adulthood. At least 100 flies per genotype were scored in more than 5 independent experiments.

For lifespan analysis, more than 100 flies per genotype were collected in individual vials containing no more than 30 flies and assayed for longevity as previously described (WITTMANN *et al.* 2001). Flies were transferred to fresh vials every other day. Lifespans were measured by scoring dead flies remaining in the old vial and plotted using the Kaplan-Meir method. The median lifespan (MedLS) was calculated as the age when half of the flies have died, and the survival distribution of two genotypic groups were compared using the log-rank (Mantel-Cox) test.

**Climbing assay**

Climbing assays were performed as previously described (RHODENIZER *et al.* 2008). Briefly, ~20 flies were gently tapped to the bottom of a plastic vial, and a picture was taken after 20 sec. This procedure was repeated 4 times with 1 min intervals between trials to allow the flies to recover from prior tapping. Climbing ability was evaluated by scoring the number of flies that failed to climb over 5 cm in each trial.

**Analysis of adult wings and eyes**

One wing per adult fly was separated from anesthetized flies, incubated in 100% ethanol for 3 min, dried, and mounted in 50% v/v Canada Balsam (Sigma-Aldrich) in methyl salicylate (Fisher Scientific). The images of eyes and dissected wings were obtained using an Olympus PD25 camera mounted on an Olympus BX40 microscope.

**Western analysis**

Adult flies were collected and frozen immediately in liquid nitrogen, and 30 adult heads were removed from bodies by vortexing and then collected. Heads were homogenized in an ice-cold stringent RIPA buffer (50 mM Tris-HCl pH 7.4, 150 mM NaCl, 0.1% SDS, 1% Triton X-100, 1% sodium deoxycholate), supplemented with protease and phosphatase inhibitor mixtures (Sigma-Aldrich), followed by sonication. Homogenates were centrifuged at 14,000×g for 20 min at 4˚C to separate supernatants (RIPA buffer-soluble fractions). Equal amounts of total proteins from each preparation were loaded and separated in NuPAGE gels (Invitrogen) and transferred to nitrocellulose membranes. After blocking, membranes were incubated at 4˚C overnight with primary antibodies. Primary antibodies used were rabbit anti-APP-Y188 (1:2000; abcam) and rabbit anti-β actin (1:2000; abcam). Membranes were then incubated with dye-coupled

secondary antibodies (goat anti-rabbit IRdye680 and goat anti-rabbit IRdye 800 from LI-COR). Signal was quantified using the Odyssey Infrared Imaging System (LI-COR bioscience).

**Histology and TUNEL analysis**

Heads from adult flies were fixed in 10% formalin, paraffinized, embedded in paraffin, and sectioned from a frontal orientation. Serial sections (4 μm) spanning the entire brain were collected and placed on glass slides and subjected to further analysis. Brain morphology was evaluated by staining paraffin sections with hematoxylin and eosin (H&E) as previously described (DIAS-SANTAGATA *et al.* 2007). To quantify neurodegeneration, the number of vacuoles larger than 5 μm in diameter was counted throughout the serial sections of the entire brain (usually 25-30 sections). At least 10 individual brains were analyzed per genotype for each time point.

Cells undergoing apoptosis were detected in the paraffin sections by TUNEL, according to the manufacturer's instructions (TdT Enzyme DNA Fragmentation Detection Kit; EMD Millipore, Calbiochem, FragEL). Quantification of the TUNEL-positive (TUNEL+) cells was performed by counting cells labeled with visible markers in all the serial sections (4 μm) of the entire fly brain (usually 25-30 sections). At least 11 individual brains were analyzed per genotype.

**Data availability**

The authors state that all data necessary for confirming the conclusions presented in the article are presented fully in the article. *Drosophila* strains used in this study are available upon request.

## Results

### Generation and validation of transgenic shRNA lines using a ubiquitous *Gal4* driver

We designed 3-4 distinct shRNAs against *Psn* or *Nct* using the Perl program (Figure 1A), and generated *UAS-Psn* or *UAS-Nct* shRNA transgenic flies, which permit spatial and temporal restriction of *Psn* or *Nct* inactivation using the Gal4/UAS system (BRAND and PERRIMON 1993; DIETZL *et al.* 2007; NI *et al.* 2011). Ubiquitous expression of *Psn* shRNA using the *Actin5C-Gal4* driver in *Act5c>shPsn* (*Actin5C-Gal4/+; UAS-shPsn/+*) flies caused early- to mid-pupal lethality, similar to the previous observation in *Psn*-null homozygous mutants (STRUHL and GREENWALD 1999; YE *et al.* 1999; MAHONEY *et al.* 2006). Levels of *Psn* transcripts in *Act5C>shPsn* 3rd instar larvae were significantly reduced (~80-90% depending on the specific shRNA line) compared to control flies (Figure 1B). Similar to *Act5c>shPsn* transgenic flies, *Act5C>shNct* (*Actin5C-Gal4/+; UAS-shNct/+*) transgenic flies also showed early pupal lethality, similar to *Nct*-null homozygous mutants (CHUNG and STRUHL 2001; ZHANG *et al.* 2005). Levels of *Nct* mRNA in *Act5C>shNct* 3rd instar larvae were also significantly reduced (~90%) compared to control flies (Figure 1C). Furthermore, *Psn* and *Nct* KD using two additional ubiquitous drivers, *tub-Gal4* and *en-Gal4*, also produced pupal lethality (data not shown).

### Notching wing phenotypes in *Psn* and *Nct* KD flies using a wing disc-specific *Gal4* driver

One of the most striking phenotypes of *Psn* and *Nct* loss-of-function mutant flies is the notching wing phenotype observed in the wing containing $Psn^{-/-}$ or $Nct^{-/-}$ mosaic clones (STRUHL and GREENWALD 1999; KLEIN *et al.* 2000; CHUNG and STRUHL 2001; LOPEZ-SCHIER and ST JOHNSTON 2002). Consistent with these earlier findings, notching wing phenotypes were also observed in wing disc-specific *Psn* (*c96>shPsn*) and *Nct* (*c96>shNct*) KD flies (Figure 2A),

using the wing imaginal disc driver *c96-Gal4* (GUSTAFSON and BOULIANNE 1996). We quantified the severity of the wing phenotypes to identify the most potent shRNA lines (Figure 2B, C). The strongest *shPsn* line, *shPsn2,* produced the most severe notching phenotypes with loss of wing margins in approximately 30% of the *c96>shPsn2* flies (Figure 2A, C). The weaker *shPsn* lines, *shPsn4* and *shPsn1*, only showed mildly thickened veins in the wing margins (L3 for *c96>shPsn4*; L3 and L4 for *c96>shPsn1*), whereas *c96>shPsn3* flies showed thickened L2 veins in addition to L3 and L4 (Figure 2A). Similar to *c96>shPsn* flies, *c96>shNct* flies also showed thickened veins in the L3 and L4 wing margins (*c96>shNct1*), and severe notching with blistered phenotypes and loss of wing margins (*c96>shNct2* and *c96>shNct3*) (Figure 2A, C). These results indicate that these *UAS-shPsn* and *UAS-shNct* lines effectively knockdown *Psn* and *Nct* expression and function. Since the *UAS-shPsn2* and *UAS-shNct2* lines are most effective, we selected them for further extensive analysis. We also included the *UAS-shPsn3* and *UAS-shNct3* lines in further studies to rule out possible off-target effects of *shPsn2* and *shNct2*.

**Early mortality, climbing defects and rough eyes in neuron-specific *Psn* KD flies**

To examine the consequences of neuron-specific *Psn* and *Nct* KD, we used the *elav-Gal4* driver to express *shPsn* and *shNct* in neurons beginning at embryonic stages (YAO and WHITE 1994). We found that *elav>shPsn2* flies show pupal lethality in males. At 25ºC, all *elav>shPsn2* flies were females (83/219) and no males eclosed from 219 pupae (Figure 3B), likely due to the stronger Gal4 expression in males (KOUSHIKA *et al.* 1996). Among *elav>shPsn2* female escapers, ~65% (114/177) showed normal expanded wings and ~35% (63/177) showed wrinkled wings (Figure 3C). qRT-PCR analysis of 3rd instar larvae revealed that relative to the control, levels of *Psn* mRNA are reduced by ~34% in whole larvae and ~75% in dissected larval brains of *elav>shPsn2* (Figure 3A). In adult *elav>shPsn2* female escapers, qRT-PCR showed ~20% and

~65% reduction of *Psn* mRNA levels in the whole body and the head, respectively (Figure 3A). The remaining *Psn* mRNA detected in whole larvae or dissected larval brains and adult flies or heads is largely due to normal *Psn* expression in non-neuronal cells where *shPsn2* is not expressed.

Next, we evaluated locomotor function using a well-established climbing assay (FEANY and BENDER 2000; AL-RAMAHI *et al.* 2007; RHODENIZER *et al.* 2008). Adult *elav>shPsn2* females with normal expanded wings at 3 days of age showed a severe defect in climbing ability (Figure 3D). Furthermore, the lifespan of *elav>shPsn2* female escapers with either wrinkled or expanded wings was drastically reduced (Figure 3E). At 25ºC culture conditions, most of *elav>shPsn2* female escapers with wrinkled wings died before 10 days (Figure 3E), and the maximum (~58 days) and median (~22 days) lifespan of *elav>shPsn2* female escapers with normal wings were significantly reduced compared to control flies ($p$<0.0001, Mantel-Cox test; Figure 3E and Table 1). The *elav>shPsn2* female escapers also exhibited rough eye phenotypes compared to control flies (Figure 3F).

**Similar but less severe phenotypes associated with another *Psn* RNAi line**

To confirm the specificity of the phenotypes of *elav>shPsn2* flies (i.e., that they are not caused by off-target effects of the hairpin used), we tested an additional shRNA line against *Psn* (*UAS-shPsn3*) which targets the last exon of the *Psn* coding region. A lower score in wing margin defects of *c96>shPsn3* relative to *c96>shPsn2* (Figure 2C) suggested that *shPsn3* is less effective. Indeed, we were able to obtain male *elav>shPsn3* adult flies (33/117), albeit at a reduced number, in contrast to *elav>shPsn2* (0/219), whereas female *elav>shPsn3* flies were obtained at a normal ratio (59/117). Together, the pupa-to-adult viability of *elav>shPsn3* flies

was significantly decreased (~21%) compared to controls (Figure 4B). Thus, two independent *shPsn* lines in *elav>shPsn* caused pupal lethality in a dose-dependent manner.

qRT-PCR analysis showed that *Psn* mRNA levels are reduced in the adult head of *elav>shPsn3* male escapers (~82%) and female flies (~54%) (Figure 4A). Climbing tests revealed that *elav>shPsn3* flies also exhibit defects in locomotion in both males and females (Figure 4C). Furthermore, similar to *elav>shPsn2*, *elav>shPsn3* also showed significantly earlier mortality in male escapers (MaxLS=55 days, MedLS=23 days; $p<0.0001$; Figure 4D and Table 1) and female flies (MaxLS=81 days, MedLS=62 days; $p<0.0001$; Figure 4E and Table 1) compared to control flies (male: MaxLS=96 days, MedLS=62 days; female: MaxLS=99 days, MedLS=87 days). Lastly, similar to *elav>shPsn2*, the male *elav>shPsn3* escapers also exhibit severe rough eyes, a phenotype that is 100% penetrant (Figure 4F), whereas female *elav>shPsn3* flies have normal compound eyes (Figure 4G).

**Phenotypic rescues of neuron-specific *Psn* KD using a fly *Psn* transgene**

To determine whether the phenotypes observed in *elav>shPsn* flies can be rescued by human *PSEN1* or fly *Psn* transgenes, we first used two independent lines of human *UAS-hPSEN1* (BL33811 and BL33812). Neuron-specific expression of either wild-type human *PSEN1* transgene in *elav>hPSEN1* flies did not cause any detectable phenotypes in male lethality, wing expansion or eye roughness (Figure 5A). Furthermore, neither of the *hPSEN1* transgenes in *elav>shPsn2, hPSEN1* flies was able to rescue any of the phenotypes associated with *elav>shPsn2* flies, such as male lethality, wrinkled wings and rough eyes in the female escapers (Figure 5A). This lack of rescue may reflect that human PSEN1 is less efficient in participating in the *Drosophila* γ-secretase complex.

Next, we tested *UAS-Psn+14* (BL63243), a transgenic line expressing wild-type fly *Psn*, which exhibits rough eyes in males and females (YE and FORTINI 1999). The *Psn+14* line was able to rescue significantly the pupa-to-adult viability of *elav>shPsn2* male flies (Figure 5C). At 25ºC, we were able to obtain male *elav>shPsn2, Psn+14* adult flies from pupae (4/32), in contrast to *elav>shPsn2* (0/56), whereas female flies were obtained at normal ratios, *elav>shPsn2, Psn+14* (16/32) and *elav>shPsn2* (26/56). The pupa-to-adult viability of *elav>shPsn2, Psn+14* flies was still significantly reduced (~36%), compared to controls (Figure 5C). While the rough eye and the wrinkled wing phenotypes associated with *elav>shPsn2* female flies were rescued in *elav>shPsn2, Psn+14* female flies (Figure 5B, D), *elav>shPsn2, Psn+14* male flies still exhibited these phenotypes (Figure 5B, D). Thus, the phenotypes observed in *Psn* KD flies, which could be rescued by expression of a fly *Psn* transgene, are due to loss of Psn function instead of off-target effects of *shPsn2*.

**Similar phenotypes exhibited by two independent lines of neuron-specific *Nct* KD flies**

We further tested two independent *UAS-shNct* lines using the *elav-Gal4* driver to determine whether *elav>shNct* flies exhibit similar phenotypes as those observed in *elav>shPsn* flies. Interestingly, *elav>shNct2* flies showed even more severe phenotypes relative to *elav>shPsn* flies. At 25ºC, no males and only 11 females eclosed from 225 *elav>shNct2* pupae (Figure 6B). qRT-PCR analysis of *elav>shNct2* 3$^{rd}$ instar larvae revealed that levels of *Nct* mRNA are reduced by ~36% in whole larvae and ~64% in dissected larval brains relative to the controls (Figure 6A). The remaining *Nct* mRNA detected in whole larvae or larval brains is largely due to normal *Nct* expression in non-neuronal cells where *shNct* is not expressed. Climbing tests revealed that *elav>shNct2* flies exhibit severe defects in locomotion in the female

escapers (Figure 6C), and all female *elav>shNct2* flies died within 7 days. In addition, all female escapers showed wrinkled wings and rough eye phenotypes (Figure 6G).

Similar to *elav>shNct2*, *elav>shNct3* flies also showed severe pupal lethality with no males and only 13 females eclosing from 95 pupae (Figure. 6E). qRT-PCR analysis of *elav>shNct3* 3rd instar larvae showed reduced levels of *Nct* mRNA in whole larvae (~42%) and in dissected larval brains (~64%) relative to controls (Figure 6D). Furthermore, *elav>shNct3* female escapers exhibited severe climbing defects (Figure 6F) and rough eyes (Figure 6H), and all died within 10 days.

These findings together demonstrate that neuron-specific *Psn* or *Nct* KD severely impairs development, resulting in pupal to early adult lethality. We therefore decided to impose temporal restriction of *Psn* or *Nct* KD to adult neurons to bypass the requirement of Psn and Nct in neural development.

**Age-dependent climbing defects and shortened lifespan in adult neuron-specific *Psn* and *Nct* cKD flies**

To restrict *Psn* or *Nct* KD to adult neurons, we used *elav-Gal4* coupled with a ubiquitously expressed temperature-sensitive allele of the Gal80 repressor (*tub-Gal80$^{ts}$*) (MA and PTASHNE 1987; MCGUIRE *et al.* 2003). The temperature sensitive Gal80 repressor under the control of the *tubulin* promoter can selectively control the binding affinity of Gal4 to the *UAS* sequence. To knockdown *Psn* expression selectively in adult neurons, we generated adult neuron specific *Psn* conditional KD flies (AN-*Psn* cKD*; elav-Gal4/y;; tub-Gal80$^{ts}$/UAS-shPsn2*). AN-*Psn* cKD and control flies (*elav-Gal4/y;; tub-Gal80$^{ts}$/+*) were cultured at a permissive temperature (22ºC) until eclosion, and then shifted to a restrictive temperature (27ºC) after metamorphosis into adults (Figure 7A). At 22ºC, AN-*Psn* cKD adult flies, examined one day

after eclosion, were obtained at normal male/female ratio (0.99±0.02), and showed no climbing defects or eye phenotypes (data not shown). Furthermore, *Psn* mRNA levels were normal in the adult heads of male AN-*Psn* cKD flies relative to controls (Figure 7B). Similarly, at 22ºC, AN-*Nct* cKD flies did not show male pupal lethality (male/female ratio=1.00±0.1), climbing defects, eye phenotypes, or reduction of *Nct* mRNA levels in the adult heads of male AN-*Nct* cKD flies relative to controls (Figure 7B). For further analysis only male flies were used, as males of *elav>shPsn3* showed greater reduction of *Psn* mRNA than females (Figure 4A).

At the restrictive temperature (27ºC), AN-*Psn* cKD and AN-*Nct* cKD flies showed significant reduction (~60%) in *Psn* or *Nct* mRNA levels in the heads of 10 day-old males (Figure 7B). Although ~40% of *Psn* or *Nct* mRNA was still detected in the head of AN-*Psn* cKD or AN-*Nct* cKD flies relative to controls, this is likely due to normal *Psn* or *Nct* expression in non-neuronal cells in the adult fly head and the reduced efficiency of Gal4 in the presence of Gal80. We then evaluated locomotor function at various ages to determine whether there is age-dependent decline in climbing ability. Climbing tests revealed that control flies showed age-dependent reduction in climbing (one-way ANOVA $F(2,15)=108.6$, $p<0.0001$, Figure 7C). While AN-*Psn* cKD and AN-*Nct* cKD flies at 10 and 30 days of age performed comparably to control flies in the climbing test, AN-*Psn* cKD and AN-*Nct* cKD flies at 50 days of age performed significantly worse relative to control flies ($p<0.0001$, Figure 7C). A two-way ANOVA showed main effects of genotype ($F(2, 45)=6.471$; $p=0.0034$) and ages ($F(2, 45)=556.1$; $p<0.0001$) with an interaction between these factors ($F(4, 45)=9.905$; $p<0.0001$).

The lifespan of AN-*Psn* cKD flies was significantly decreased (MaxLS=63 days, MedLS=46 days; $p<0.0001$) compared to controls (MaxLS=69 days, MedLS=53 days; Figure. 7D). Similarly, the lifespan of AN-*Nct* cKD flies was also significantly decreased (MaxLS=62

days, MedLS=46 days; $p<0.0001$) compared to controls (MaxLS=67 days, MedLS=51 days; Figure. 7E). Importantly, AN-*Psn/Nct* cKD (*elav-Gal4/y;; tub-Gal80$^{ts}$, UAS-shPsn2/UAS-shNct2)* flies, which knocked down both *Psn* and *Nct* in adult neurons, showed an even greater reduction in lifespan (MaxLS=46 days, MedLS=32 days; $p<0.0001$) compared to AN-*Psn* cKD and AN-*Nct* cKD (Figure 7F).

**Reduced γ-secretase activity in adult neuron-specific *Psn* cKD flies**

To evaluate γ-secretase activity in AN-*Psn* cKD flies, we used the Gal4/UAS and LexA/LexAop system to express selectively in adult neurons the APP-LV chimeric protein, in which the full length human APP is fused to the LexA DNA-binding domain and the VP16 activator domain (LV) (LOEWER *et al.* 2004). APP-LV is cleaved to generate the APP intracellular domain (AICD) and LV (AICD-LV) fusion fragment following sequential cleavages by α- or β- and γ-secretases. The AICD-LV fragment translocates to the nucleus, and binds and activates the LexA operator, which drives the expression of a green fluorescent protein (GFP) reporter, permitting visualization of the γ-secretase-mediated cleavage event *in vivo* (Figure 7G). Western analysis of protein lysates from adult heads (3 days post eclosion) at restrictive temperature of 27ºC revealed ~30-fold accumulation of APP-CTF-LV, which is the γ-secretase substrate, in AN-*Psn* cKD; *APP$^{LV}$* flies (*elav-Gal4/y; LexAop-hrGFP/+; tub-Gal$^{80}$, UAS-shPsn2/UAS-APP$^{LV}$*) relative to controls (*elav-Gal4/y; LexAop-hrGFP/+; tub-Gal$^{80}$/UAS-APP$^{LV}$*), indicating severe impairment of γ-secretase activity (Figure 7H, I). Consistent with the biochemical findings, GFP signals were also diminished in AN-*Psn* cKD; *APP$^{LV}$* brains relative to controls.

**Age-dependent neurodegeneration in adult neuron-specific *Psn* and *Nct* cKD flies**

To determine the impact of *Psn* or *Nct* KD in neurons of the adult brain during aging, we performed histological analysis of AN-*Psn, -Nct* and -*Psn/Nct* cKD flies at multiple ages. Examination by H&E staining revealed age-dependent increases of neuropil vacuolization in the adult brains of AN-*Psn, -Nct* and -*Psn/Nct* cKD flies compared to controls (Figure 8A). Quantification of the total number of large vacuoles (≥5 μm) present in the cortex and neuropil of AN-*Psn, -Nct* and -*Psn/Nct* cKD flies at the age of 10, 20, 30, 40 and 50 days revealed age-dependent increases of large vacuoles compared to the brains of control flies (Figure 8B). While the number of large vacuoles is not significantly increased in the AN-*Psn* and AN-*Nct* cKD brains at 20 days of age compared to control brains (two-way ANOVA with Dunnett's post-hoc), AN-*Psn/Nct* cKD brains exhibited significant increases in large vacuoles (Figure 8). This is likely due to further reduction of active γ-secretase complexes in AN-*Psn/Nct* cKD brains, relative to AN-*Psn* and AN-*Nct* cKD brains, because both *Psn* and *Nct* mRNA are 90% reduced in neurons of AN-*Psn/Nct* cKD brains. Beginning at 30 days, both AN-*Psn* and AN-*Nct* cKD brains showed significant increases in large vacuoles relative to control brains, and the number of vacuoles was even higher in AN-*Psn/Nct* cKD brains (Figure 8). By 50 days of age, the neurodegeneration phenotype was more severe in AN-*Psn* and AN-*Nct* cKD brains, and all AN-*Psn/Nct* cKD flies died before the age of 50 days. Two-way ANOVA showed main effects of genotype ($F(3, 197)=22.77$; $p<0.0001$) and age ($F(4, 197)=57.92$; $p<0.0001$) with an interaction between these factors ($F(12, 197)=19.94$; $p<0.0001$). These neuropathology results show that neuronal reduction of Psn and/or Nct in adult flies results in age-dependent and dose-related neurodegenerative changes in the adult brain.

To evaluate whether neurons undergo apoptosis in AN-*Psn*, -*Nct* and -*Psn/Nct* cKD adult brains, we performed TUNEL staining on 30 day-old flies. The number of TUNEL-positive cells

in AN-*Psn*, -*Nct* and -*Psn/Nct* cKD brains is significantly increased compared to control brains (number of TUNEL+ cells per brain: control, 15.5 ± 1.6; AN-*Psn* cKD, 47.6 ± 3.6; AN-*Nct* cKD, 50.6 ± 7.3; AN-*Psn/Nct* cKD, 64.17 ± 4.2; $p<0.0001$; $n \geq 11$ per each genotype; Figure 9). These data demonstrate that adult neuron-specific knockdown of *Psn* or *Nct* indeed causes increased apoptotic death in the brain.

## Discussion

Mutations in the *PSEN* genes account for ~90% of the identified FAD mutations, and it has been proposed that *PSEN* mutations cause FAD *via* a loss-of-function mechanism (SHEN and KELLEHER 2007). FAD *PSEN* mutations are mostly missense mutations (>260) scattered throughout the coding sequence. Genetic studies in mice have demonstrated that Presenilins are essential for synaptic function, learning and memory, and age-dependent neuronal survival (YU *et al.* 2001; BEGLOPOULOS *et al.* 2004; FENG *et al.* 2004; SAURA *et al.* 2004; ZHANG *et al.* 2009; WINES-SAMUELSON *et al.* 2010; WATANABE *et al.* 2014). Furthermore, studies using cultured cells and knockin mice have shown that FAD *PSEN* mutations are loss-of-function mutations, causing reduced γ-secretase activity and recapitulating phenotypes of knockout mice (HEILIG *et al.* 2010; HEILIG *et al.* 2013; XIA *et al.* 2015; XIA *et al.* 2016).

In the current study, we investigated whether *Drosophila* Psn is also required for neuronal survival in the aging fly brain. We circumvented the pupal lethality associated with germline *Psn* loss-of-function mutants by generating conditional KD flies expressing *Psn* shRNA selectively in neurons of the adult brain. Using a ubiquitous driver, we first confirmed that our *Psn* shRNA lines result in 80-90% reduction of mRNA levels (Figure 1) and recapitulate developmental phenotypes of *Psn* germ-line mutant flies (STRUHL and GREENWALD 1999; YE *et*

*al.* 1999; CHUNG and STRUHL 2001; MAHONEY *et al.* 2006). Consistent with notching wings in *Notch* heterozygous mutant flies and in wing-specific *Notch* or *Psn* KD flies (BOYLES *et al.* 2010; CASSO *et al.* 2011), wing disc-specific expression of *Psn* shRNA leads to similar wing phenotypes at varying severity, allowing selection of the most effective *Psn* shRNA line (Figure 2). Selective neuronal expression of two independent *Psn* shRNA lines beginning at embryonic stages caused earlier lethality, rough eye phenotypes, and severe climbing defects (Figures 3, 4), and these phenotypes were partially rescued by expressing a *Drosophila Psn* transgene (Figure 5). Further restriction of *Psn* shRNA expression to adult neurons using the *elav-Gal4/tub-Gal80$^{ts}$* system bypassed developmental phenotypes associated with *elav>shPsn* flies, and resulted in age-dependent climbing defects, shortened lifespan and impairment of γ-secretase activity (Figure 7), age-dependent neurodegeneration (Figure 8) and elevated cell death in the adult brain (Figure 9). Therefore, *Drosophila* Psn is also required for neuronal survival in the aging brain as well as normal lifespan and behavior, demonstrating that the essential role of PS in neuronal protection during aging is evolutionarily conserved from fruit flies to mammals.

*Drosophila Psn* models have previously provided significant insight into the normal physiological function of Psn. Impairment of synaptic plasticity and associated learning and memory has been reported in *Psn*-null mutant larvae (KNIGHT *et al.* 2007). Heterozygous *Psn* loss-of-function mutant flies displayed age-dependent learning and memory deficits at old ages without any loss of neurons from TUNEL analysis or gross defects in the mushroom body, suggesting that heterozygosity of *Psn* in flies is insufficient to cause neurodegeneration (MCBRIDE *et al.* 2010). These findings are consistent with our previous report showing that *Psen1* cKO mice exhibit impairment in spatial learning and memory in the absence of neurodegeneration (YU *et al.* 2001). Transgenic flies expressing *Psn* FAD mutations under the

endogenous *Psn* promoter in a *Psn*-null background showed severe developmental phenotypes including pupal lethality and notching wings, similar to those of *Psn* loss-of-function mutant flies, indicating that these FAD mutations cause loss of Psn function (SEIDNER *et al.* 2006). In addition, large-scale genetic screens in flies with *Psn* hypomorphic alleles using Notch-like developmental phenotypes in the eye and wing identified genetic modifiers of the Notch pathway (MAHONEY *et al.* 2006). Another screen in flies with Notch-related phenotypes using *Psn* overexpression in notum and wing recovered modifiers involved in the regulation of Psn activity, calcium signaling and Notch signaling (VAN DE HOEF *et al.* 2009). While Presenilin regulates neurogenesis via Notch signaling in the developing mouse brain (SONG *et al.* 1999; HANDLER *et al.* 2000; KIM and SHEN 2008), PS-dependent neuronal survival in the aging brain is Notch-independent, as inactivation of both Notch1 and Notch2 in excitatory neurons of the postnatal forebrain does not cause neurodegeneration (ZHENG *et al.* 2012).

In addition to PS, genetic studies of another γ-secretase component Nct, in mice also demonstrated the essential role of Nct in learning and memory, synaptic function and neuronal survival during aging, highlighting the importance of γ-secretase in these processes relevant to AD pathogenesis (TABUCHI *et al.* 2009; LEE *et al.* 2014). We therefore developed multiple *Drosophila shNct* lines and tested them in parallel with *shPsn* lines using ubiquitous or cell type-specific drivers. Similar to *Psn* KD flies, selective *Nct* KD in wing discs resulted in notching wing phenotypes, whereas earlier lethality, climbing defects and rough eyes were observed in neuron-specific *Nct* KD flies (Figures 2, 6). Furthermore, selective *Nct* KD in adult neurons caused age-dependent climbing defects and shortened lifespan (Figure 7), age-dependent neurodegeneration (Figure 8) and elevated cell death in the adult brain (Figure 9). These phenotypes were more severe in adult neuron-specific *Psn/Nct* double cKD flies (Figures 7-9),

likely due to further reduction of functional γ-secretase complexes and thereby its activity. Consistent with genetic findings from analysis of *PS* cDKO and *Nct* cKO mice (BEGLOPOULOS *et al.* 2004; SAURA *et al.* 2004; TABUCHI *et al.* 2009; WINES-SAMUELSON *et al.* 2010), the findings from the current *Drosophila* study provide further evidence for the importance of PS and Nct in the promotion of neuronal survival during aging, highlighting the evolutionary conservation of this pathway in the protection of the aging brain.

A recent report in *C. elegans* described mitochondrial morphology defects and elevated cytosolic calcium levels in *sel-12* loss-of-function mutants (SARASIJA and NORMAN 2015). Indeed, *PS* cDKO mice exhibit age-dependent reduction of mitochondrial density and selective increases of larger mitochondria in cortical neurons at 6 months of age (WINES-SAMUELSON *et al.* 2010). Presenilin plays a key role in the regulation of calcium homeostasis but the regulatory site by PS has been hotly debated because of varying experimental systems employed in the studies (HO and SHEN 2011). Using physiologically relevant experimental systems, such as the hippocampus of *PS* cDKO mice and primary dissociated hippocampal neurons lacking PS, we previously reported that PS modulates presynaptic short-term plasticity through its regulation of ryanodine receptor-mediated calcium release from the ER (ZHANG *et al.* 2009; WU *et al.* 2013). Future studies in adult neuron-specific *Psn* and *Nct* fly models using calcium and cell death reporters could provide insight into how calcium dysregulation may be involved in neuronal cell death *in vivo*.

Despite the importance of Presenilin in promoting neuronal survival in the aging brain, the underlying molecular pathway remains unknown. This is partly due to the fact that only 0.1% of excitatory neurons lacking PS in the cerebral cortex undergo apoptosis at a given time (WINES-SAMUELSON *et al.* 2010), making it challenging to study the molecular mechanisms

underlying neuronal death in these cells. These unique adult neuron-specific *Psn* and *Nct* cKD fly models will permit a functional, genetic dissection to identify downstream targets of PS and physiological substrates of γ-secretase that mediate neuronal survival during aging, which may be further explored as novel therapeutic targets for Alzheimer's disease.

## Acknowledgements

We thank M. Feany and G. Struhl for their advice during this project, and Bloomington *Drosophila* Stock Center for providing fly stocks. We are grateful for the technical support provided by the staff at the *Drosophila* RNAi Screening Center, R. Binari, C. Hu, and members of the Shen and Perrimon labs for discussion. This work was supported by grants from the NIH (R01NS041783, R01NS042818, R01NS101745 to J.S.) and an award from the MetLife Foundation. N.P. is an investigator of the Howard Hughes Medical Institute.

## References


AL-RAMAHI, I., A. M. PEREZ, J. LIM, M. ZHANG, R. SORENSEN *et al.*, 2007 dAtaxin-2 mediates expanded Ataxin-1-induced neurodegeneration in a Drosophila model of SCA1. PLoS Genet **3:** e234.

BAI, X. C., C. YAN, G. YANG, P. LU, D. MA *et al.*, 2015 An atomic structure of human gamma-secretase. Nature **525:** 212-217.

BEGLOPOULOS, V., X. SUN, C. A. SAURA, C. A. LEMERE, R. D. KIM *et al.*, 2004 Reduced beta-amyloid production and increased inflammatory responses in presenilin conditional knock-out mice. J Biol Chem **279:** 46907-46914.

BOYLES, R. S., K. M. LANTZ, S. POERTNER, S. J. GEORGES and A. J. ANDRES, 2010 Presenilin controls CBP levels in the adult Drosophila central nervous system. PLoS One **5:** e14332.

BRAND, A. H., and N. PERRIMON, 1993 Targeted gene expression as a means of altering cell fates and generating dominant phenotypes. Development **118:** 401-415.

CASSO, D. J., B. BIEHS and T. B. KORNBERG, 2011 A novel interaction between hedgehog and Notch promotes proliferation at the anterior-posterior organizer of the Drosophila wing. Genetics **187:** 485-499.

CHUNG, H. M., and G. STRUHL, 2001 Nicastrin is required for Presenilin-mediated transmembrane cleavage in Drosophila. Nat Cell Biol **3:** 1129-1132.

DE STROOPER, B., W. ANNAERT, P. CUPERS, P. SAFTIG, K. CRAESSAERTS *et al.*, 1999 A presenilin-1-dependent gamma-secretase-like protease mediates release of Notch intracellular domain. Nature **398:** 518-522.

DIAS-SANTAGATA, D., T. A. FULGA, A. DUTTAROY and M. B. FEANY, 2007 Oxidative stress mediates tau-induced neurodegeneration in Drosophila. J Clin Invest **117:** 236-245.

DIETZL, G., D. CHEN, F. SCHNORRER, K. C. SU, Y. BARINOVA *et al.*, 2007 A genome-wide transgenic RNAi library for conditional gene inactivation in Drosophila. Nature **448:** 151-156.

DONOVIEL, D. B., A. K. HADJANTONAKIS, M. IKEDA, H. ZHENG, P. S. HYSLOP *et al.*, 1999 Mice lacking both presenilin genes exhibit early embryonic patterning defects. Genes Dev **13:** 2801-2810.

FEANY, M. B., and W. W. BENDER, 2000 A Drosophila model of Parkinson's disease. Nature **404:** 394-398.

FENG, R., H. WANG, J. WANG, D. SHROM, X. ZENG *et al.*, 2004 Forebrain degeneration and ventricle enlargement caused by double knockout of Alzheimer's presenilin-1 and presenilin-2. Proc Natl Acad Sci U S A **101:** 8162-8167.

GROTH, A. C., M. FISH, R. NUSSE and M. P. CALOS, 2004 Construction of transgenic Drosophila by using the site-specific integrase from phage phiC31. Genetics **166:** 1775-1782.

GUSTAFSON, K., and G. L. BOULIANNE, 1996 Distinct expression patterns detected within individual tissues by the GAL4 enhancer trap technique. Genome **39:** 174-182.

HANDLER, M., X. YANG and J. SHEN, 2000 Presenilin-1 regulates neuronal differentiation during neurogenesis. Development **127:** 2593-2606.

HEILIG, E. A., U. GUTTI, T. TAI, J. SHEN and R. J. KELLEHER, 3RD, 2013 Trans-dominant negative effects of pathogenic PSEN1 mutations on gamma-secretase activity and Abeta production. J Neurosci **33:** 11606-11617.

HEILIG, E. A., W. XIA, J. SHEN and R. J. KELLEHER, 3RD, 2010 A presenilin-1 mutation identified in familial Alzheimer disease with cotton wool plaques causes a nearly complete loss of gamma-secretase activity. J Biol Chem **285:** 22350-22359.

HO, A., and J. SHEN, 2011 Presenilins in synaptic function and disease. Trends Mol Med **17:** 617-624.

HONG, C. S., and E. H. KOO, 1997 Isolation and characterization of Drosophila presenilin homolog. Neuroreport **8:** 665-668.

HU, Y., Y. YE and M. E. FORTINI, 2002 Nicastrin is required for gamma-secretase cleavage of the Drosophila Notch receptor. Dev Cell **2:** 69-78.

KIM, W. Y., and J. SHEN, 2008 Presenilins are required for maintenance of neural stem cells in the developing brain. Mol Neurodegener **3:** 2.

KLEIN, T., L. SEUGNET, M. HAENLIN and A. MARTINEZ ARIAS, 2000 Two different activities of Suppressor of Hairless during wing development in Drosophila. Development **127:** 3553-3566.

KNIGHT, D., K. ILIADI, M. P. CHARLTON, H. L. ATWOOD and G. L. BOULIANNE, 2007 Presynaptic plasticity and associative learning are impaired in a Drosophila presenilin null mutant. Dev Neurobiol **67:** 1598-1613.

KOUSHIKA, S. P., M. J. LISBIN and K. WHITE, 1996 ELAV, a Drosophila neuron-specific protein, mediates the generation of an alternatively spliced neural protein isoform. Curr Biol **6:** 1634-1641.

LEE, S. H., M. SHARMA, T. C. SUDHOF and J. SHEN, 2014 Synaptic function of nicastrin in hippocampal neurons. Proc Natl Acad Sci U S A **111:** 8973-8978.

LEVY-LAHAD, E., W. WASCO, P. POORKAJ, D. M. ROMANO, J. OSHIMA *et al.*, 1995 Candidate gene for the chromosome 1 familial Alzheimer's disease locus. Science **269:** 973-977.

LI, Y. M., M. XU, M. T. LAI, Q. HUANG, J. L. CASTRO *et al.*, 2000 Photoactivated gamma-secretase inhibitors directed to the active site covalently label presenilin 1. Nature **405:** 689-694.

LOEWER, A., P. SOBA, K. BEYREUTHER, R. PARO and G. MERDES, 2004 Cell-type-specific processing of the amyloid precursor protein by Presenilin during Drosophila development. EMBO Rep **5:** 405-411.

LOPEZ-SCHIER, H., and D. ST JOHNSTON, 2002 Drosophila nicastrin is essential for the intramembranous cleavage of notch. Dev Cell **2:** 79-89.

LUKINOVA, N. I., V. V. ROUSSAKOVA and M. E. FORTINI, 1999 Genetic characterization of cytological region 77A-D harboring the presenilin gene of Drosophila melanogaster. Genetics **153:** 1789-1797.

MA, J., and M. PTASHNE, 1987 The carboxy-terminal 30 amino acids of GAL4 are recognized by GAL80. Cell **50:** 137-142.

MAHONEY, M. B., A. L. PARKS, D. A. RUDDY, S. Y. TIONG, H. ESENGIL *et al.*, 2006 Presenilin-based genetic screens in Drosophila melanogaster identify novel notch pathway modifiers. Genetics **172:** 2309-2324.

MARKSTEIN, M., C. PITSOULI, C. VILLALTA, S. E. CELNIKER and N. PERRIMON, 2008 Exploiting position effects and the gypsy retrovirus insulator to engineer precisely expressed transgenes. Nat Genet **40:** 476-483.

MCBRIDE, S. M., C. H. CHOI, B. P. SCHOENFELD, A. J. BELL, D. A. LIEBELT *et al.*, 2010 Pharmacological and genetic reversal of age-dependent cognitive deficits attributable to decreased presenilin function. J Neurosci **30:** 9510-9522.

MCGUIRE, S. E., P. T. LE, A. J. OSBORN, K. MATSUMOTO and R. L. DAVIS, 2003 Spatiotemporal rescue of memory dysfunction in Drosophila. Science **302:** 1765-1768.

NGUYEN, V., C. HAWKINS, C. BERGERON, A. SUPALA, J. HUANG *et al.*, 2006 Loss of nicastrin elicits an apoptotic phenotype in mouse embryos. Brain Res **1086:** 76-84.

NI, J. Q., R. ZHOU, B. CZECH, L. P. LIU, L. HOLDERBAUM *et al.*, 2011 A genome-scale shRNA resource for transgenic RNAi in Drosophila. Nat Methods **8:** 405-407.

RHODENIZER, D., I. MARTIN, P. BHANDARI, S. D. PLETCHER and M. GROTEWIEL, 2008 Genetic and environmental factors impact age-related impairment of negative geotaxis in Drosophila by altering age-dependent climbing speed. Exp Gerontol **43:** 739-748.

ROGAEV, E. I., R. SHERRINGTON, E. A. ROGAEVA, G. LEVESQUE, M. IKEDA *et al.*, 1995 Familial Alzheimer's disease in kindreds with missense mutations in a gene on chromosome 1 related to the Alzheimer's disease type 3 gene. Nature **376:** 775-778.

SARASIJA, S., and K. R. NORMAN, 2015 A gamma-Secretase Independent Role for Presenilin in Calcium Homeostasis Impacts Mitochondrial Function and Morphology in Caenorhabditis elegans. Genetics **201:** 1453-1466.

SAURA, C. A., S. Y. CHOI, V. BEGLOPOULOS, S. MALKANI, D. ZHANG *et al.*, 2004 Loss of presenilin function causes impairments of memory and synaptic plasticity followed by age-dependent neurodegeneration. Neuron **42:** 23-36.

SCHELLENBERG, G. D., 1995 Genetic dissection of Alzheimer disease, a heterogeneous disorder. Proc Natl Acad Sci U S A **92:** 8552-8559.

SEIDNER, G. A., Y. YE, M. M. FARADAY, W. G. ALVORD and M. E. FORTINI, 2006 Modeling clinically heterogeneous presenilin mutations with transgenic Drosophila. Curr Biol **16:** 1026-1033.

SHEN, J., R. T. BRONSON, D. F. CHEN, W. XIA, D. J. SELKOE *et al.*, 1997 Skeletal and CNS defects in Presenilin-1-deficient mice. Cell **89:** 629-639.

SHEN, J., and R. J. KELLEHER, 3RD, 2007 The presenilin hypothesis of Alzheimer's disease: evidence for a loss-of-function pathogenic mechanism. Proc Natl Acad Sci U S A **104:** 403-409.

SONG, W., P. NADEAU, M. YUAN, X. YANG, J. SHEN *et al.*, 1999 Proteolytic release and nuclear translocation of Notch-1 are induced by presenilin-1 and impaired by pathogenic presenilin-1 mutations. Proc Natl Acad Sci U S A **96:** 6959-6963.

STRUHL, G., and I. GREENWALD, 1999 Presenilin is required for activity and nuclear access of Notch in Drosophila. Nature **398:** 522-525.

TABUCHI, K., G. CHEN, T. C. SUDHOF and J. SHEN, 2009 Conditional forebrain inactivation of nicastrin causes progressive memory impairment and age-related neurodegeneration. J Neurosci **29:** 7290-7301.

VAN DE HOEF, D. L., J. HUGHES, I. LIVNE-BAR, D. GARZA, M. KONSOLAKI *et al.*, 2009 Identifying genes that interact with Drosophila presenilin and amyloid precursor protein. Genesis **47:** 246-260.

VENKEN, K. J., Y. HE, R. A. HOSKINS and H. J. BELLEN, 2006 P[acman]: a BAC transgenic platform for targeted insertion of large DNA fragments in D. melanogaster. Science **314:** 1747-1751.

VERT, J. P., N. FOVEAU, C. LAJAUNIE and Y. VANDENBROUCK, 2006 An accurate and interpretable model for siRNA efficacy prediction. BMC Bioinformatics **7:** 520.

WATANABE, H., M. IQBAL, J. ZHENG, M. WINES-SAMUELSON and J. SHEN, 2014 Partial loss of presenilin impairs age-dependent neuronal survival in the cerebral cortex. J Neurosci **34:** 15912-15922.

WINES-SAMUELSON, M., E. C. SCHULTE, M. J. SMITH, C. AOKI, X. LIU *et al.*, 2010 Characterization of age-dependent and progressive cortical neuronal degeneration in presenilin conditional mutant mice. PLoS One **5:** e10195.

WITTMANN, C. W., M. F. WSZOLEK, J. M. SHULMAN, P. M. SALVATERRA, J. LEWIS *et al.*, 2001 Tauopathy in Drosophila: neurodegeneration without neurofibrillary tangles. Science **293:** 711-714.

WU, B., H. YAMAGUCHI, F. A. LAI and J. SHEN, 2013 Presenilins regulate calcium homeostasis and presynaptic function via ryanodine receptors in hippocampal neurons. Proc Natl Acad Sci U S A **110:** 15091-15096.

XIA, D., R. J. KELLEHER, 3RD and J. SHEN, 2016 Loss of Abeta43 Production Caused by Presenilin-1 Mutations in the Knockin Mouse Brain. Neuron **90:** 417-422.

XIA, D., H. WATANABE, B. WU, S. H. LEE, Y. LI *et al.*, 2015 Presenilin-1 knockin mice reveal loss-of-function mechanism for familial Alzheimer's disease. Neuron **85:** 967-981.

YAO, K. M., and K. WHITE, 1994 Neural specificity of elav expression: defining a Drosophila promoter for directing expression to the nervous system. J Neurochem **63:** 41-51.

YE, Y., and M. E. FORTINI, 1999 Apoptotic activities of wild-type and Alzheimer's disease-related mutant presenilins in Drosophila melanogaster. J Cell Biol **146:** 1351-1364.

YE, Y., N. LUKINOVA and M. E. FORTINI, 1999 Neurogenic phenotypes and altered Notch processing in Drosophila Presenilin mutants. Nature **398:** 525-529.

YU, G., M. NISHIMURA, S. ARAWAKA, D. LEVITAN, L. ZHANG *et al.*, 2000 Nicastrin modulates presenilin-mediated notch/glp-1 signal transduction and betaAPP processing. Nature **407:** 48-54.

YU, H., C. A. SAURA, S. Y. CHOI, L. D. SUN, X. YANG *et al.*, 2001 APP processing and synaptic plasticity in presenilin-1 conditional knockout mice. Neuron **31:** 713-726.

ZHANG, C., B. WU, V. BEGLOPOULOS, M. WINES-SAMUELSON, D. ZHANG *et al.*, 2009 Presenilins are essential for regulating neurotransmitter release. Nature **460:** 632-636.

ZHANG, T., S. TRAN, C. CLOUSER and F. PIGNONI, 2005 Nicastrin controls aspects of photoreceptor neuron specification and differentiation in the Drosophila eye. Dev Dyn **234:** 590-601.

ZHENG, J., H. WATANABE, M. WINES-SAMUELSON, H. ZHAO, T. GRIDLEY *et al.*, 2012 Conditional deletion of Notch1 and Notch2 genes in excitatory neurons of postnatal forebrain does not cause neurodegeneration or reduction of Notch mRNAs and proteins. J Biol Chem **287:** 20356-20368.

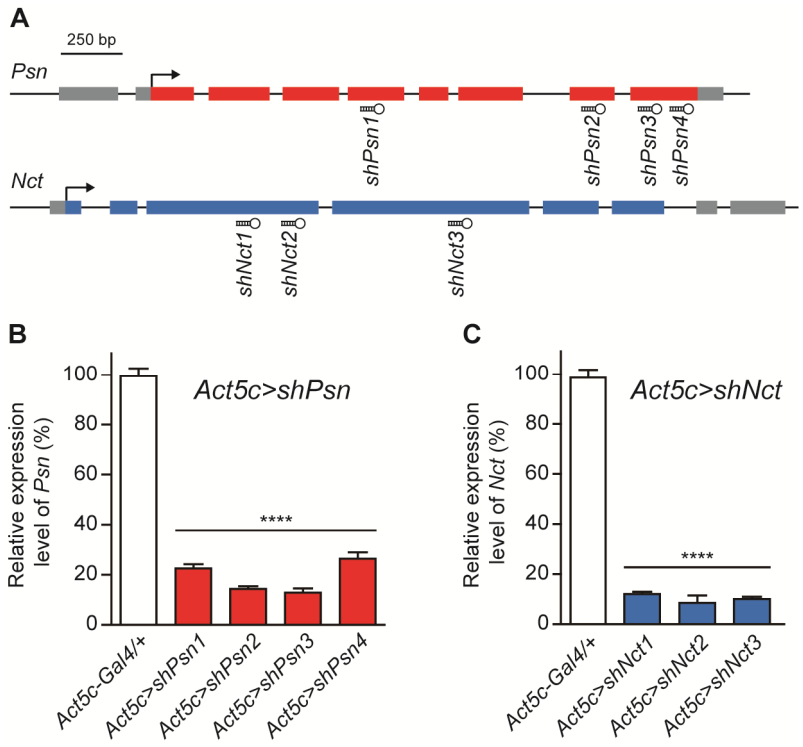


**Figure 1. Generation and validation of *UAS-shPsn* and *UAS-shNct* transgenic lines using a ubiquitous *Gal4* driver**

(**A**) Schematic gene structures of *Psn* and *Nct* and the target regions of the *Psn* and *Nct* shRNAs. Grey boxes indicate the 5'- or 3'-UTR. Colored boxes indicate exons. Hairpins indicate the shRNAs and the corresponding target regions. (**B, C**) Ubiquitous expression of all of the *Psn* and *Nct* shRNAs using the *Act5c-Gal4* driver result in pupal lethality and ~80-90% reduction of mRNA levels in *Act5c>shPsn* and *Act5c>shNct* whole 3$^{rd}$ instar larvae, compared to control (*Act5c-Gal4/+*). qRT-PCR analysis of *Psn* (**B**) and *Nct* (**C**) mRNA levels was performed using total RNA extracted from five whole 3$^{rd}$ instar larvae per genotype. *Psn* and *Nct* mRNA levels were normalized to *rp49* mRNA levels as internal control. n=4 independent experiments. All data are expressed as mean ± SEM. Statistical analysis was performed using one-way ANOVA with Dunnett's post-hoc comparisons, ****$p$<0.0001.

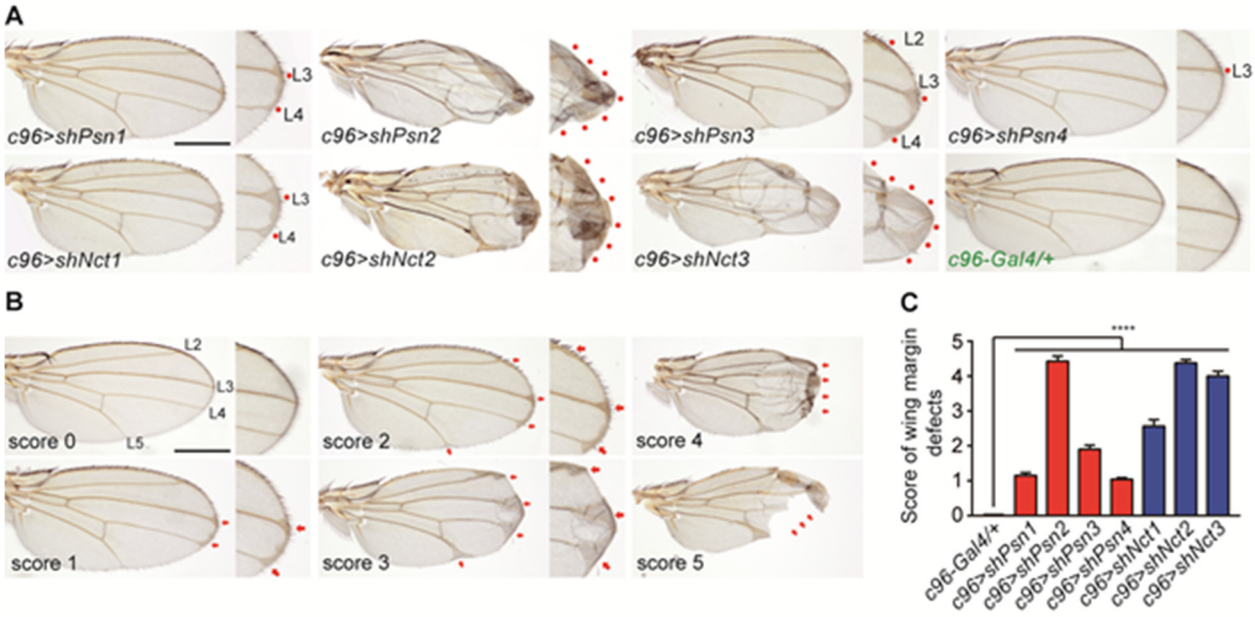


**Figure 2. Notching wing phenotypes in wing-specific *Psn* and *Nct* KD flies**

(**A**) Expression of *shPsn* or *shNct* under the control of the *c96-Gal4* driver results in thickened veins and/or notching wing margins. Representative adult wing images of control (*c96-Gal4/+*) and wing-specific *Psn* (*c96>shPsn*) or *Nct* (*c96>shNct*) KD flies are shown. The wing margin is also shown in higher magnification views. Red dots mark thickened veins or blistered phenotypes in the wing margins. Scale bar: 0.5 mm. (**B**) Representative adult wing images used to establish the scoring system for quantifying the severity of the wing phenotypes. Score 0: wild-type wing morphology. Score 1: mildly thickened L3 and L4 veins near the margin. Score 2: thickened L2, L3, L4 and L5 veins near the margin. Score 3: more enhanced vein phenotypes. Score 4: severe vein and blistered phenotypes. Score 5: severe margin loss. (**C**) Quantification of the severity of wing phenotypes using the scoring system shown in (**B**). At least 20 wings were scored per genotype. All data are expressed as mean ± SEM. Statistical analysis was performed using one-way ANOVA with Dunnett's post-hoc comparisons, ****$p$<0.0001.

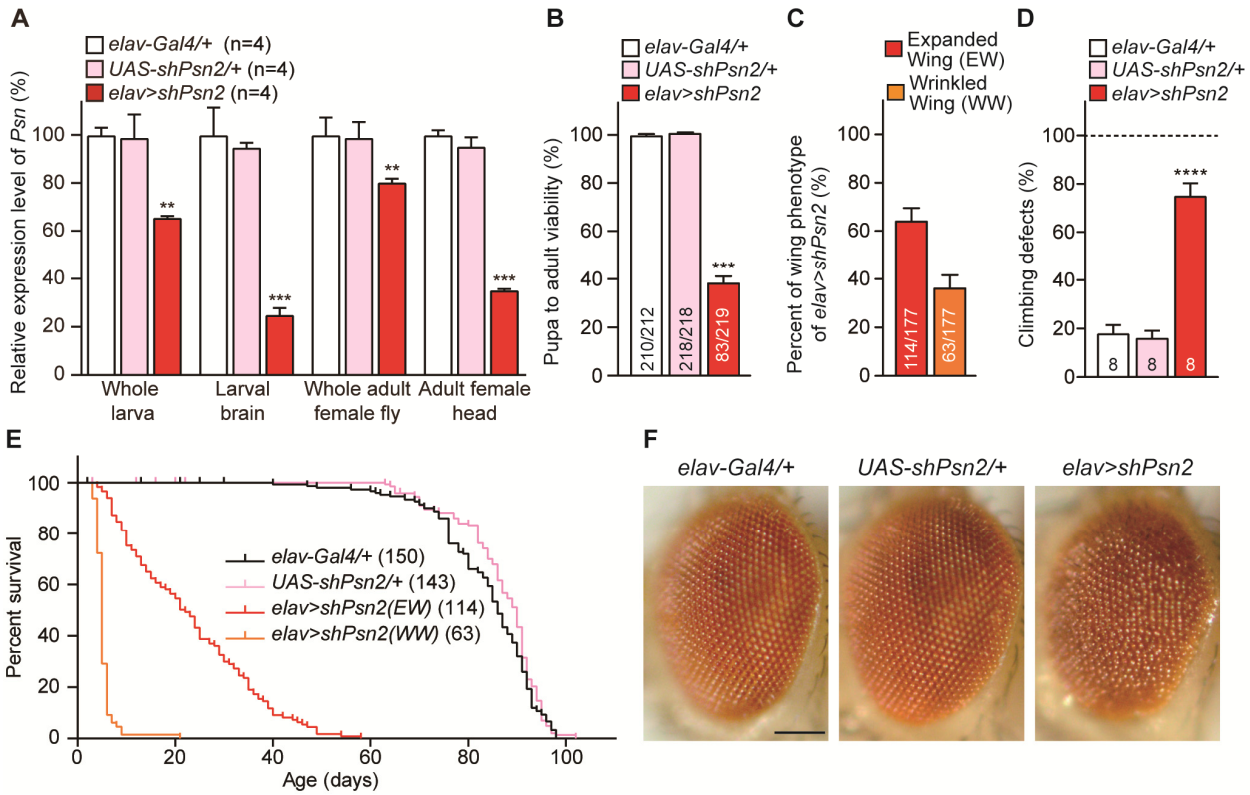


**Figure 3. Severe early mortality, climbing defects and rough eyes in *elav>shPsn* flies**

(**A**) Significant reduction of *Psn* mRNA level in *elav>shPsn2*. qRT-PCR analysis of *Psn* mRNA levels in 3rd instar larvae (whole larvae or dissected brains) or 3 day-old adults (whole flies or heads only). *Psn* mRNA levels were normalized to *rp49* mRNA levels as internal control. Total RNA was extracted from whole larvae (5 larvae per genotype), larval brains (15 brains per genotype), whole adult females (5 adults per genotype) or adult female heads only (20 heads per genotype). n=4 independent experiments. (**B**) Neuron-specific KD of *Psn* reduces pupa-to-adult viability. Viability was calculated by dividing the total number of flies by the total number of pupae, and shown as the percentage of pupae surviving to adulthood. No male flies eclosed from *elav>shPsn2* pupae (0/219), and the number of adult females (83/219) were lower than anticipated. n=11 independent experiments; ≥210 flies per genotype (~20 flies per experiment) were used in the study. (**C**) Neuron-specific *Psn* KD results in defects on wing expansion. Percentage of *elav>shPsn2* flies with expanded or wrinkled wing phenotypes. 63.9 ± 5.6 % of *elav>shPsn2* flies had normal expanded wings (EW; red) and 36.1 ± 5.6 % of flies had wrinkled wings (WW; orange). n=4 independent experiments. (**D**) Neuron-specific *Psn* KD causes defects in climbing ability. Only *elav>shPsn2* females with normal expanded wings were used for the climbing assay. Bar indicates percentage of failed climbers. Age=3 days, n=8 independent experiments; ≥150 flies per genotype (~20 flies per experiment) were used in the study. (**E**) Neuron-specific *Psn* KD causes severe mortality. Survival of Gal4 control (*elav-Gal4/+*, black), UAS control (*UAS-shPsn2/+*, pink), and neuron-specific *Psn* KD flies (*elav-Gal4/+;; UAS-shPsn2/+*) with expanded wings (EW, red) and wrinkled wings (WW, orange). Lifespans were

plotted by the Kaplan-Meir method. (**F**) Neuron-specific *Psn* KD causes rough eye phenotypes. Representative images of the control and *ealv>shPsn2* eyes are shown Scale bar: 0.1 mm. All data are expressed as mean ± SEM. Statistical analysis was performed using one-way ANOVA with Dunnett's post-hoc comparisons. ***p*<0.01; ****p*<0.001; *****p*<0.0001.

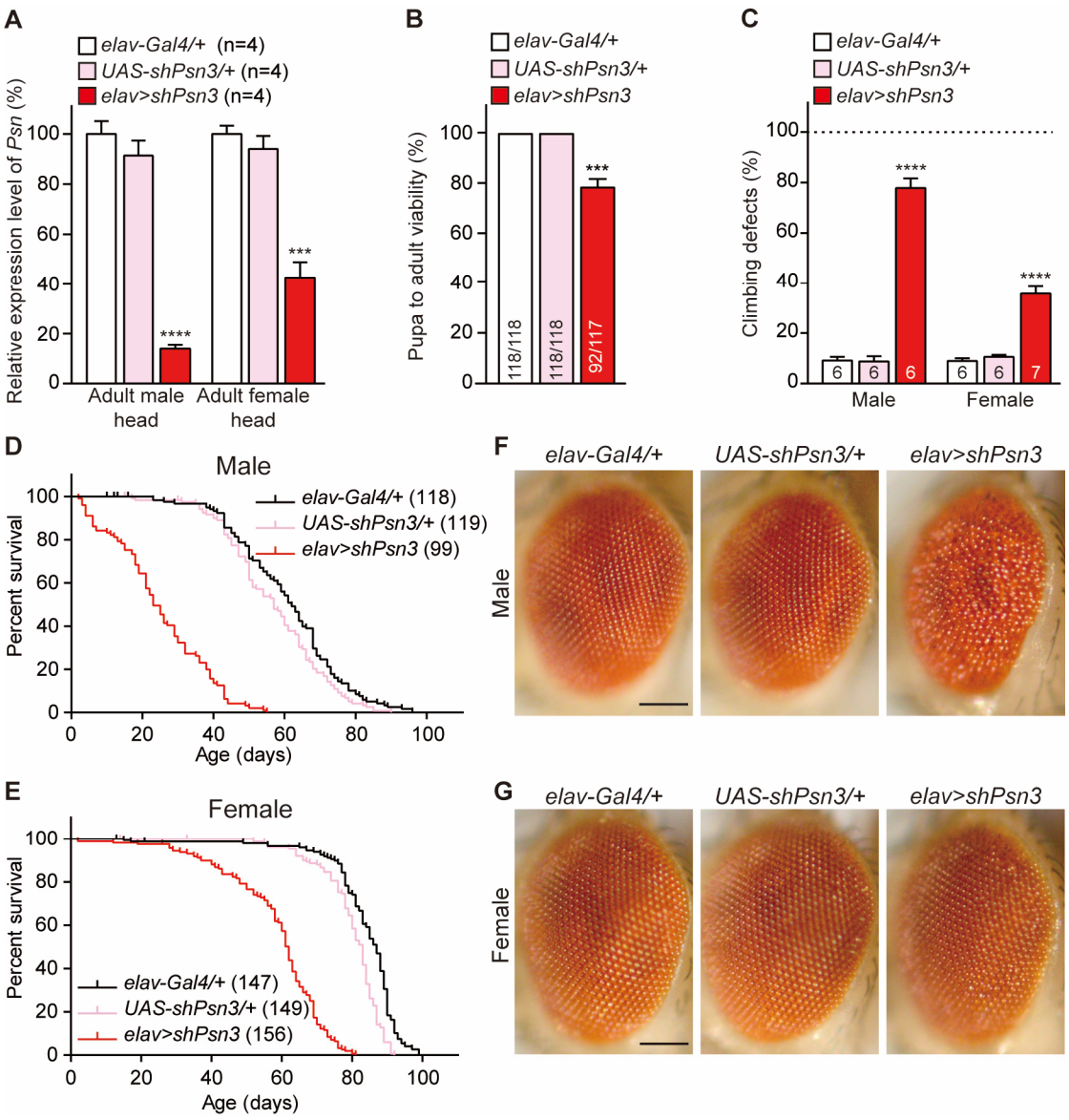


**Figure 4. Similar but less severe phenotypes associated with a different *Psn* shRNA line**

(**A**) Neuron-specific *Psn* KD using a different shRNA line results in significant reduction of *Psn* mRNA levels in 3 day-old adult heads of *elav>shPsn3* males (83±3.2%) and females (54±2.8%), compared to controls. qRT-PCR analysis of *Psn* mRNA level in adult fly heads expressing *shPsn3*. *Psn* mRNA levels are normalized to *rp49* mRNA levels as internal control. Total RNA was extracted from 20 adult heads per genotype. n=4 independent experiments. (**B**) Neuron-specific *Psn* KD in *elav>shPsn3* reduces pupa-to-adult viability (92/117). Viability was calculated by dividing the total number of flies by the total number of pupae, and shown as the percentage of pupae surviving to adulthood. n=6 independent experiments, ≥110 flies per genotype (~20 flies per experiment). (**C**) *elav>shPsn3* causes defects in climbing ability in both males and females. Bar indicates percentage of failed climbers. Age=3 days, n=6 independent experiments, ≥110 flies per genotype (~20 flies per experiment). (**D, E**) *elav>shPsn3* causes

severe mortality in male (**D**) and female (**E**) flies. Survival of *Gal4* controls (*elav-Gal4/+*, black), *UAS* controls (*UAS-shPsn3/+,* pink), and *elav>shPsn3* flies (*elav-Gal4/+;; UAS-shPsn3/+*, red). Lifespans were plotted using the Kaplan-Meir method. (**F**) *elav>shPsn3* male flies exhibit severe rough eye phenotypes. (**G**) In contrast to females with a stronger *shPsn2* line (*elav>shPsn2*), females of *elav>shPsn3* show normal compound eyes. Representative images showing adult eye of controls and *elav>shPsn3* flies. Scale bar: 0.1 mm. All data are expressed as mean ± SEM. Statistical analysis was performed using one-way ANOVA with Dunnett's post-hoc comparisons. ***$p<0.001$, ****$p<0.0001$.

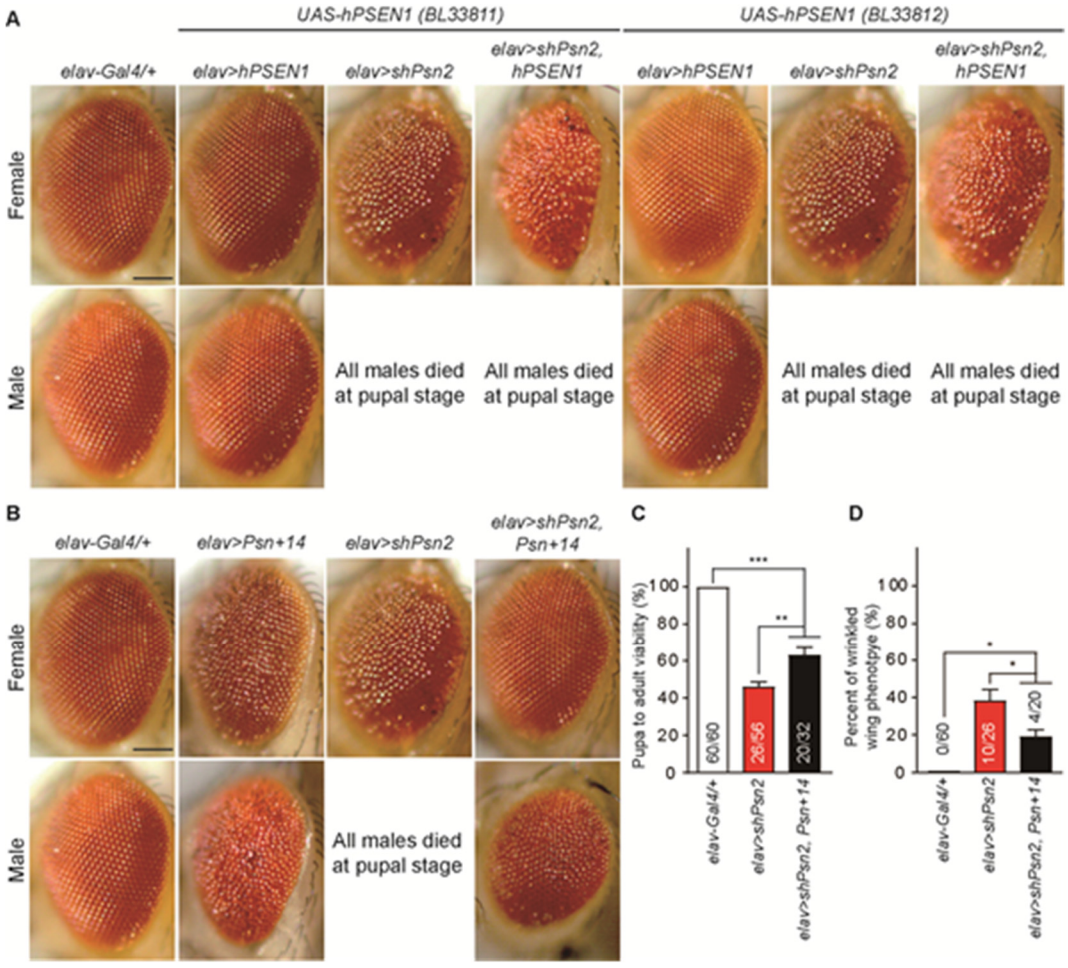


**Figure 5. Partial phenotypic rescue of neuron-specific *Psn* KD using a *Drosophila Psn* transgene**

(**A**) The *UAS-hPSEN1* transgenic lines (BL33811 and BL33812) are not able to rescue the male pupal lethality or rough eye phenotype of *elav>shPsn2*. Representative images show the adult eye of each genotype. Scale bar: 0.1 mm (**B-D**) Using a *Drosophila Psn* transgenic line, *UAS-Psn+14* (BL63243), the male pupal lethality, rough eye phenotype and defective wing expansion in *elav>shPsn2* are rescued. (**B**) Both male and female of *elav>Psn+14* show rough eye phenotypes. *elav>shPsn2, Psn+14* female flies show full rescue of the rough eye phenotype exhibited in *elav>shPsn2*. Representative images of adult eye of each genotype. Scale bar: 0.1 mm (**C**) The pupa-to-adult viability is significantly rescued in *elav>shPsn2, Psn+14* (20/32; $p<0.01$) compared to *elav>shPsn2* (26/56). However, *elav>shPsn2, Psn+14* flies showed reduced viability compared to control ($p<0.001$). Viability was calculated by dividing the total number of flies by the total number of pupae, and shown as the percentage of pupae surviving to adulthood. n=3 independent experiments. (**D**) The wrinkled wing phenotype of *elav>shPsn2* is significantly rescued in *elav>shPsn2, Psn+14* ($p<0.05$). Specifically, female *elav>shPsn2, Psn+14* flies showed normal wing phenotypes, while male *elav>shPsn2, Psn+14* flies showed wrinkled wing phenotypes. Percentage of wrinkled wing phenotypes was calculated by dividing

the number of flies with wrinkled wings by the total number of flies. All data are expressed as mean ± SEM. Statistical analysis was performed using one-way ANOVA with Tukey's post-hoc comparisons. *$p$<0.05, **$p$<0.01, ***$p$<0.001.

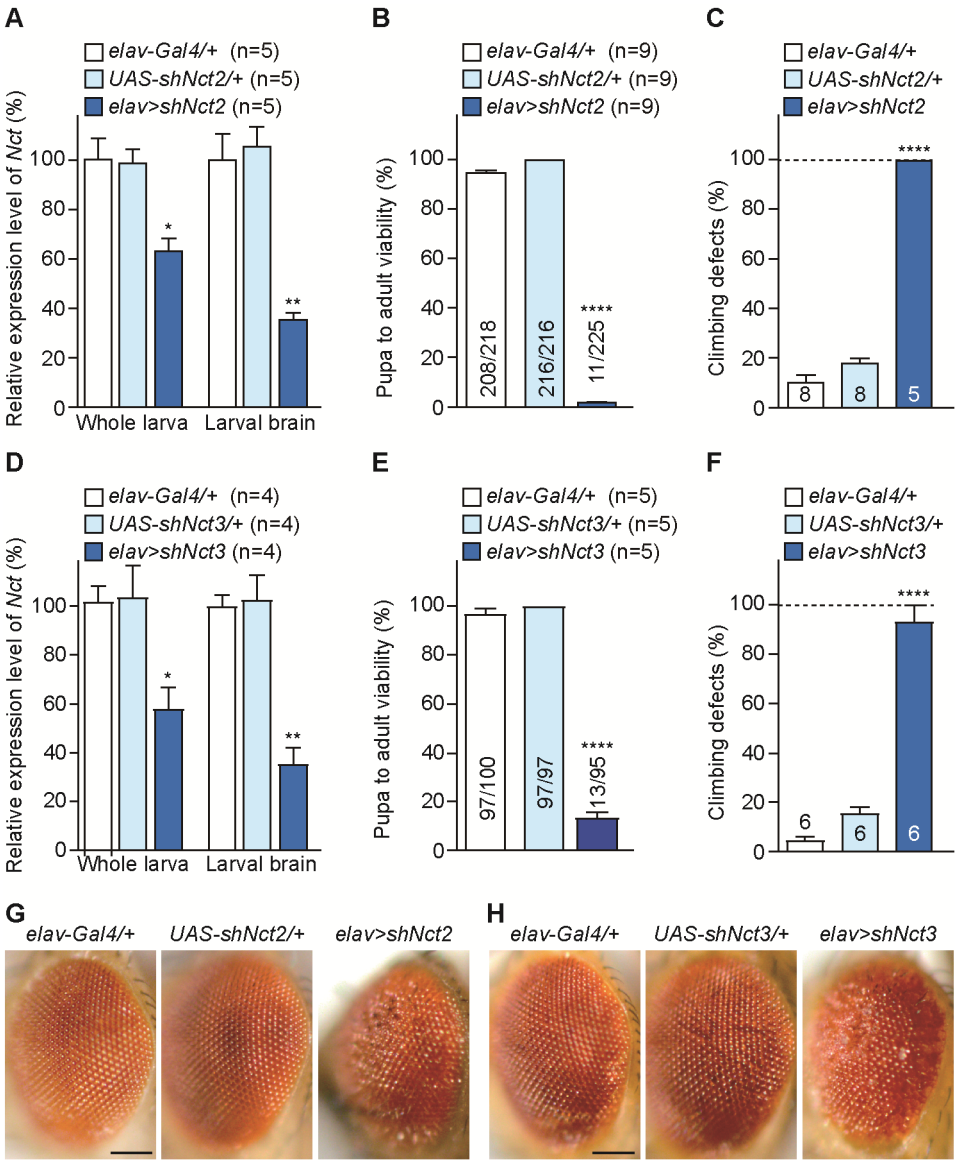


**Figure 6. Severe early mortality, climbing defects and rough eyes in *elav>shNct* flies**

(**A** and **D**) Neuron-specific *Nct* KD using two independent lines, *UAS-shNct2* (**A**) and *UAS-shNct3* (**D**), results in significant reduction of *Nct* mRNA levels in 3rd instar larvae compared to controls. qRT-PCR analysis of *Nct* mRNA level in 3rd instar larvae (whole larvae or dissected brains) of *elav>shNct2* (**A**) and *elav>shNct3* (**D**). *Nct* mRNA levels are normalized to *rp49* mRNA levels as internal control. Total RNA was extracted from whole larvae (5 larvae per genotype) or larval brains (15 brains per genotype). n=4-5 independent experiments. (**B** and **E**) Neuron-specific *Nct* KD results in decreased pupa-to-adult viability. Viability was calculated by dividing the total number of flies by the total number of pupae, and shown as the percentage of pupae surviving to adulthood. (**B**) Only 11 females *elav>shNct2* eclosed from 225 pupae. n=9 independent experiments. Total numbers of flies tested: *elav-Gal4/+*=218, *UAS-shNct2/+*=216, and *elav>shNct2*=225 (20 flies per experiment). (**E**) Only 13 females *elav>shNct3* eclosed from

95 pupae. n=5 independent experiments. Total numbers of flies tested: *elav-Gal4/+*=100, *UAS-shNct3/+*=97, and *elav>shNct3*=95 (20 flies per experiment). (**C** and **F**) Neuron-specific *Nct* KD causes defects in climbing ability. Bar indicates percentage of failed climbers. Age=3 days. Gal4 and UAS controls: n=6-8 independent experiments, ≥110 flies per genotype (20 flies per experiment). *elav>shNct2*: n=5 flies (**C**) and *elav>shNct3*: n=14 flies (**F**). (**G** and **H**) Females of both *elav>shNct2* (**G**) and *elav>shNct3* (**H**) exhibit rough eye phenotypes. Representative images showing the adult eye of each genotype. Scale bar: 0.1 mm All data are expressed as mean ± SEM. Statistical analysis was performed using one-way ANOVA with Dunnett's post-hoc comparisons. *$p$<0.05, **$p$<0.01, ****$p$<0.0001

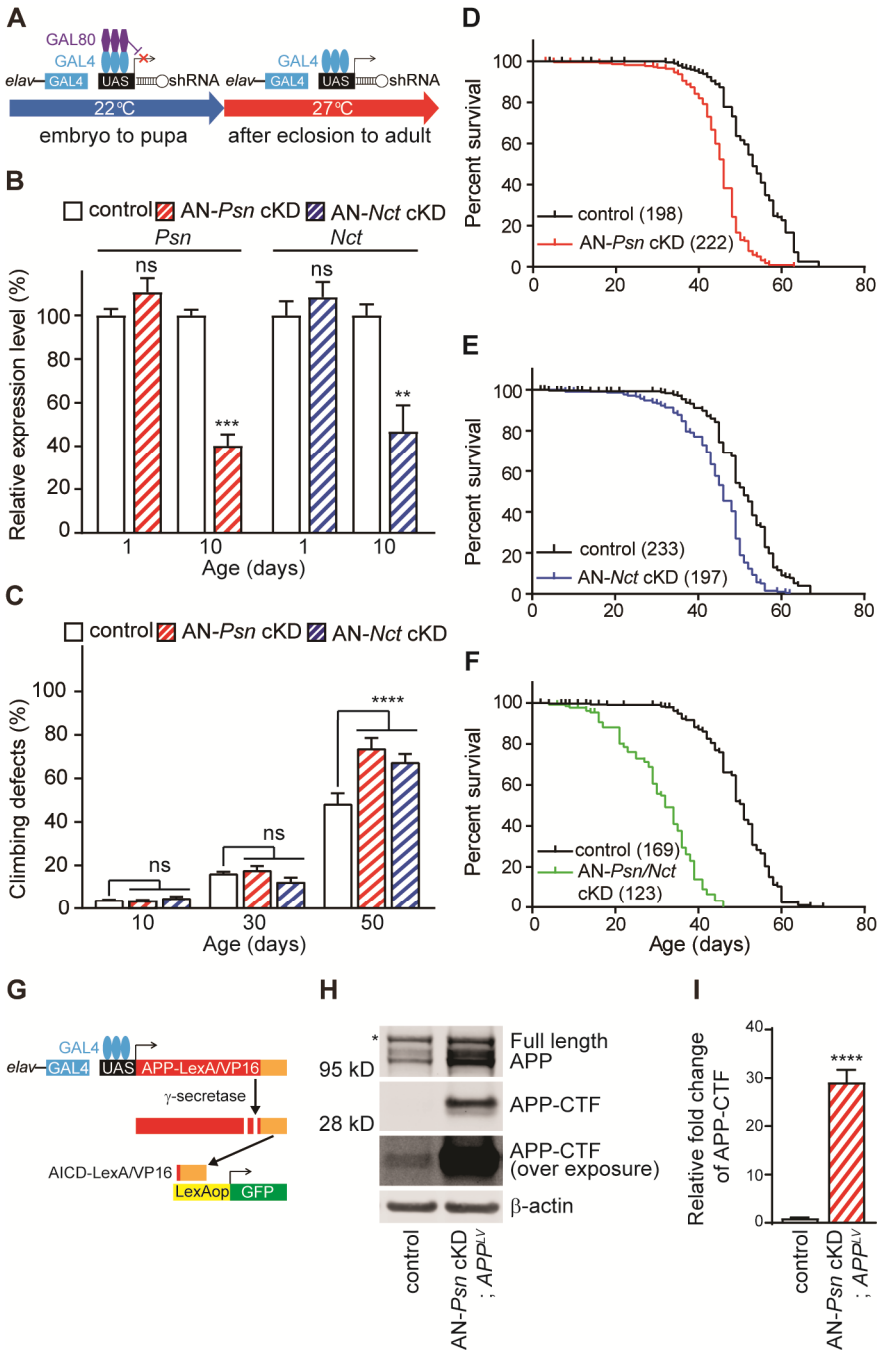


**Figure 7. Age-dependent climbing defects and shortened lifespan in adult neuron-specific *Psn* and *Nct* KD flies**

(**A**) Strategy for imposing temporal control of shRNA expression using Gal80$^{ts}$. (**B**) Adult neuron-specific conditional KD of *Psn* (AN-*Psn* cKD; red) and *Nct* (AN-*Nct* cKD; blue) results in significant reduction of *Psn* (red) or *Nct* (blue) mRNA level in 10 day-old male fly heads, but no significant difference in 1 day-old male fly heads compared to control. qRT-PCR analysis of *Psn* and *Nct* mRNA level in the male adult heads of 1 and 10 day-old flies. Total RNA was extracted from 20 male adult heads. *Psn* and *Nct* mRNA levels were normalized to *rp49* mRNA

levels as internal control. n=4 independent experiments. All data are expressed as mean ± SEM. Statistical analysis was performed using one-way ANOVA with Dunnett's post-hoc comparisons. **$p$<0.01, ***$p$<0.001. (**C**) Adult neuron-specific *Psn* or *Nct* KD causes defects in climbing ability at the age of 50 days. Bar indicates percentage of failed climbers. n≥5 independent experiments, ≥100 flies per genotype (20 flies per experiment). All data are expressed as mean ± SEM. Statistical analysis was performed using two-way ANOVA with Dunnett's post-hoc comparisons. Two-way ANOVA showed main effects of genotype ($F(2, 45)=6.471$; $p=0.0034$) and age ($F(2, 45)=556.1$; $p<0.0001$) with an interaction between these factors ($F(4, 45)=9.905$; $p<0.0001$). ns, non-significant; ****$p$<0.0001. (**D-F**) Adult neuron-specific *Psn* and *Nct* cKD reduce lifespan. AN-*Psn/Nct* cKD flies showed a greater reduced lifespan relative to AN-*Psn* cKD and AN-*Nct* cKD flies. Survival of control (black), AN-*Psn* cKD (red, **D**), AN-*Nct* cKD (blue, **E**), and AN-*Psn/Nct* cKD (green, **F**). Lifespans were plotted by the Kaplan-Meir method. (**G-I**) Impairment of γ-secretase activity in AN-*Psn* cDK flies. (**G**) Strategy for assessing γ-secretase dependent cleavage of the APP-LV reporter system. (**H**) Western analysis shows dramatic increases of γ-secretase substrate APP-CTF in the adult head of male AN-*Psn* cKD; $APP^{LV}$ flies, indicating reduction of γ-secretase activity. β-actin was used as loading control. Asterisk marks nonspecific band. (**I**) Quantification of APP-CTF levels in AN-*Psn* cKD; $APP^{LV}$ and control fly heads. APP-CTFs levels were normalized to β-actin and full length APP protein. n=3 independent experiments. All data are expressed as mean ± SEM. Statistical analysis was performed using unpaired Student *t*-test. ****$p$<0.0001.

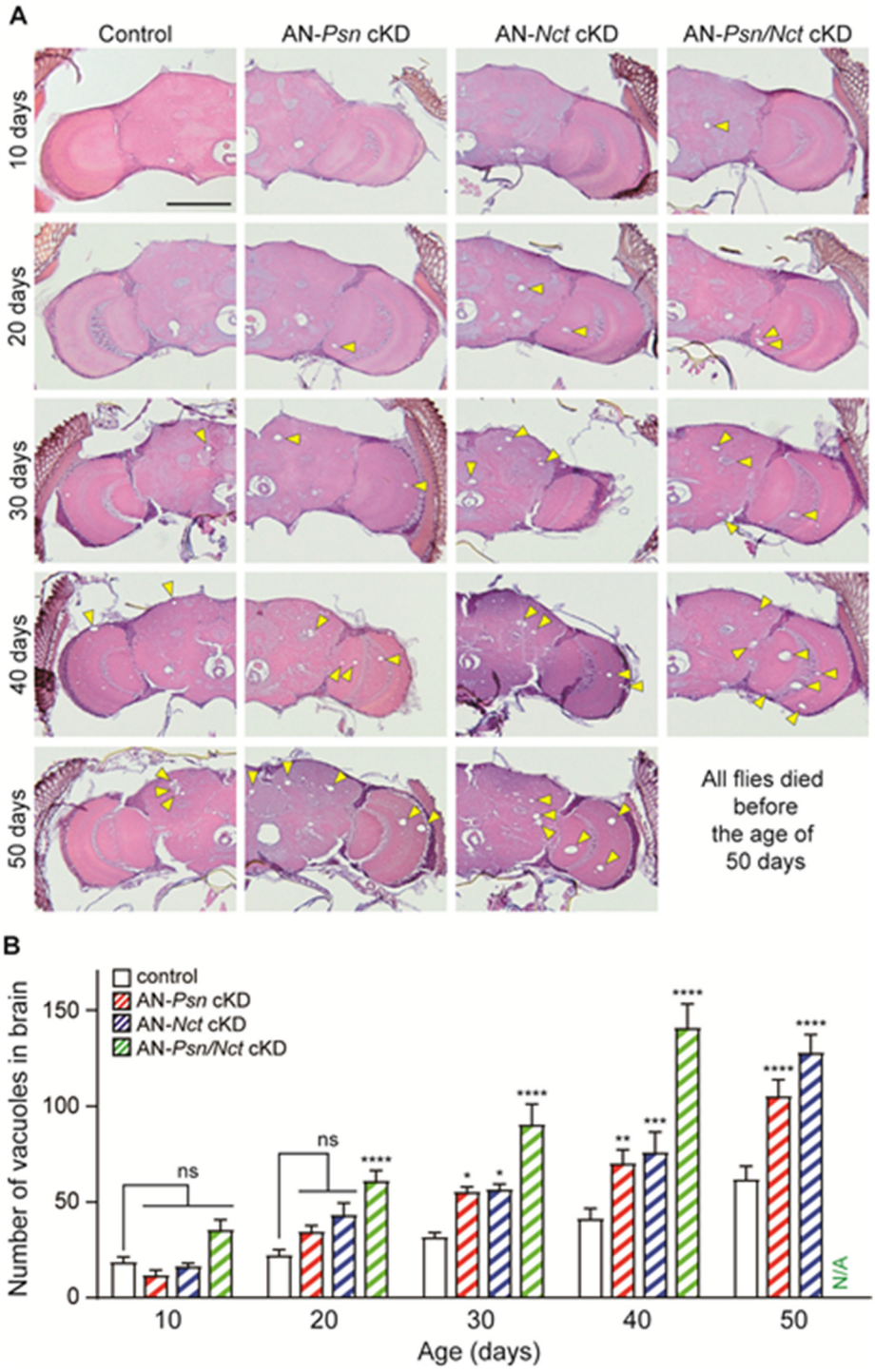


**Figure 8. Age-dependent neurodegeneration in adult neuron-specific *Psn* and *Nct* cKD flies**

(**A**) H&E staining in frontal brain sections revealed age-dependent neurodegeneration. Increased number of vacuoles (marked by arrows) indicates neurodegeneration in the brain. Scale bar: 100 μm. (**B**) Quantification of vacuoles in the brain of control (*elav-Gal4/y;; tub-Gal80$^{ts}$/+*, black), AN-*Psn* cKD (*elav-Gal4/y;; tub-Gal80$^{ts}$/UAS-shPsn2,* red), AN-*Nct* cKD (*elav-Gal4/y;; tub-*

*Gal80$^{ts}$/UAS-shNct2,* blue), and AN-*Psn/Nct* cKD flies (*elav-Gal4/y;; tub-Gal80$^{ts}$, UAS-shPsn2/UAS-shNct2,* green). Neurodegeneration is minimal in the brain of control flies. The brains of AN-*Psn* cKD and -*Nct* cKD flies show significant age-dependent neurodegeneration compared to brains of control flies at the age of 30, 40 and 50 days. The brains of AN-*Psn/Nct* cKD flies show significant age-dependent neurodegeneration compared to the brains of control flies at the age of 20, 30 and 40 days. All AN-*Psn/Nct* cKD flies died before the age of 50 days. Total number of vacuoles greater than 5 μm in diameter was counted throughout all sections of entire brains. n=10-17 brains per genotype. All data are expressed as mean ± SEM. Statistical analysis was performed using two-way ANOVA with Dunnett's post-hoc comparisons. Two-way ANOVA showed main effects of genotype ($F(3, 197)=22.77$; $p<0.0001$) and age ($F(4, 197)=57.92$; $p<0.0001$) with an interaction between these factors ($F(12, 197)=19.94$; $p<0.0001$). ns, non-significant; *$p<0.05$, **$p<0.01$, ****$p<0.001$, ****$p<0.0001$.

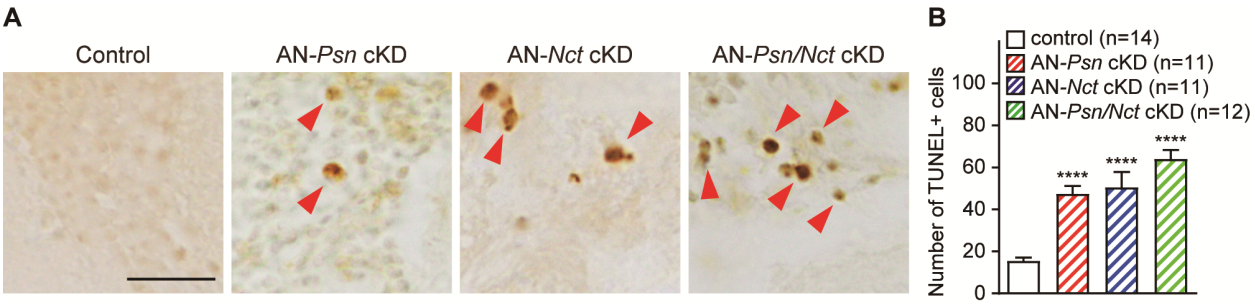


**Figure 9. Increased apoptosis in the brain of adult neuron-specific *Psn* and *Nct* cKD flies**

(**A**) Apoptotic cells (marked by arrows) were identified by TUNEL staining. Scale bar: 10 μm. (**B**) Quantification of TUNEL+ cells. The number of TUNEL+ cells is increased in AN-*Psn* cKD, AN-*Nct* cKD and AN-*Psn/Nct* cKD brains compared to control brains. n=11-14 brains per genotype at 30 days of age. All data are expressed as mean ± SEM. Statistical analysis was performed using one-way ANOVA with Dunnett's post-hoc comparisons. ****$p<0.0001$.

| Experimental group | Number of flies tested (n) | Median Lifespan (days) | % Change | χ2 | Log-rank |
|---|---|---|---|---|---|
| ***elav>shPsn2*** **(Fig. 3E)** | | | | | |
| *elav-Gal4/+* | 150 | 86 | | | |
| *+/+;; UAS-shPsn2/+* | 143 | 90 | 4.65 | 2.6 | $p$=0.1079 |
| *elav-Gal4/+;; UAS-shPsn2/+*(EW) | 114 | 22 | -75.56 | 345.7 | $p$<0.0001 |
| *elav-Gal4/+;; UAS-shPsn2/+*(WW) | 65 | 5 | -77.27 | 292.1 | $p$<0.0001 |
| ***elav>shPsn3*** **male (Fig. 4D)** | | | | | |
| *elav-Gal4/y* | 118 | 62 | | | |
| *+/y; UAS-shPsn3/+* | 119 | 56 | -9.68 | 6.902 | $p$<0.01 |
| *elav-Gal4/y; UAS-shPsn3/+* | 99 | 23 | -58.93 | 214.1 | $p$<0.0001 |
| ***elav>shPsn3*** **female (Fig. 4E)** | | | | | |
| *elav-Gal4/+* | 147 | 87 | | | |
| *+/+; UAS-shPsn3/+* | 149 | 83 | -4.60 | 36.47 | $p$<0.0001 |
| *elav-Gal4/+; UAS-shPsn3/+* | 156 | 62 | -19.48 | 284.4 | $p$<0.0001 |
| **AN-*Psn* cKD (Fig. 7D)** | | | | | |
| *elav-Gal4/y;; tub-Gal80$^{ts}$/+* (control) | 198 | 53 | | | |
| *elav-Gal4/y;; tub-Gal80$^{ts}$/UAS-shPsn2* | 222 | 46 | -13.21 | 146.4 | $p$<0.0001 |
| **AN-*Nct* cKD (Fig. 7E)** | | | | | |
| *elav-Gal4/y;; tub-Gal80$^{ts}$/+* (control) | 233 | 51 | | | |
| *elav-Gal4/y;; tub-Gal80$^{ts}$/UAS-shNct2* | 197 | 46 | -9.80 | 76.63 | $p$<0.0001 |
| **AN-*Psn/Nct* cKD (Fig. 7F)** | | | | | |
| *elav-Gal4/y;; tub-Gal80$^{ts}$/+* (control) | 169 | 51 | | | |
| *elav-Gal4/y;; tub-Gal80$^{ts}$, UAS-shPsn2/UAS-shNct2* | 123 | 32 | -37.26 | 388 | $p$<0.0001 |

**Table 1. Results and statistical analyses of lifespan using the Log-rank test**

% change shows differences in median lifespan between control and experimental groups. $p$ values were determined in each comparison between the control and the experimental group by the Mantel-Cox test.